The coordination numbers of the iron(II) and iron(III) ions are important to develop a more detailed structural model for these glasses.

5. Conclusions

A lead iron phosphate glass with composition $43.3PbO \cdot 13.7Fe_2O_3 \cdot 43P_2O_5$ (mol%), $O/P = 3.5$, has a chemical durability comparable with the best iron phosphate $40Fe_2O_3 \cdot 60P_2O_5$ glass (same O/P ratio). The O/P ratio is an important factor concerning the aqueous chemical durability. Replacement of Fe–O–P bonds for Pb–O–P bonds does not affect the chemical durability. The only crystalline phase detected after heating this glass was $Fe_2Pb(P_2O_7)_2$ while lead free iron phosphate glasses with same O/P ratio present ferric and/or ferrous pyrophosphate crystals. For the LIP glasses, the observed IR and Raman scattering spectra are representative of a mixture of chain-terminating Q^1 species and chain-forming Q^2 species. No Raman bands related to P=O vibrations and Q^0 species were observed.

From the EPR measurements it is concluded that Fe^{3+} ions are not constrained to occupy only central positions of tetrahedral and octahedral sites of the glass formers, but are also found at interstitial or peripheral positions in the glass network.

Acknowledgements

S.T.R. thanks Fapesp for the pos-doc financial support (Proc. # 00/06684-9). J.R.M. acknowledges the research financial support granted by FAPESP (Proc. # 99/08281-0). The authors are indebted to Alexandre Hamada for the IR spectra.

References

[1] B.C. Sales, L.A. Boatner, Mater. Lett. 2 (1984) 301.
[2] F. Chen, D.E. Day, Ceram. Trans. 93 (1999) 213.
[3] B.C. Sales, L.A. Boatner, Science 226 (1984) 45.
[4] S.T. Reis, J.R. Martinelli, J. Non-Cryst. Solids 247 (1999) 241.
[5] X. Fang, C.S. Ray, D.E. Day, J. Non-Cryst. Solids 263&264 (2000) 293.
[6] M.G. Mesko, D.E. Day, J. Non-Cryst. Solids 273 (1999) 27.
[7] A. Mogus-Milankovic, B. Pivac, K. Furic, D.E. Day, Phys. Chem. Glasses 38 (1997) 74.
[8] C.S. Ray, X. Fang, M. Karabulut, G.K. Marasinghe, D.E. Day, J. Non-Cryst. Solids 249 (1999) 1.
[9] R. Berger, J. Kliava, P. Beziade, J. Non-Cryst. Solids 180 (1995) 151.
[10] J. Kliava, R. Berger, J. Trokss, J. Non-Cryst. Solids 202 (1996) 205.
[11] G.K. Marasinghe, C.S. Ray, D.E. Day, J. Non-Cryst. Solids 263&264 (2000) 146.
[12] G.K. Marasinghe, M. Karabulut, C.S. Ray, D.E. Day, J. Non-Cryst. Solids 222 (2000) 144.
[13] X. Yu, D.E. Day, G.J. Long, R.K. Brow, J. Non-Cryst. Solids 215 (1997) 21.
[14] D.E. Day, Z. Wu, C.S. Ray, P. Hrma, J. Non-Cryst. Solids 241 (1998) 1.
[15] B.C. Sales, M.M. Abraham, J.B. Bates, L.A. Boatner, J. Non-Cryst. Solids 71 (1985) 103.
[16] B. Wanklyn et al., J. Mater. Sci. Lett. 2 (1983) 511.
[17] R.S. Alger, Electron Paramagnetic Resonance: Techniques and Applications, Wiley-Interscience, New York, 1968, p. 43.
[18] B.C. Bunker, G.W. Arnold, J.A. Wilder, J. Non-Cryst. Solids 64 (1984) 291.
[19] S.T. Reis, M. Karabulut, D.E. Day, J. Non-Cryst. Solids 292 (2001) 150.
[20] A. Mogus-Milankovic, D.E. Day, J. Non-Cryst. Solids 162 (1993) 275.
[21] R.K. Brow, T.M. Alam, D.R. Tallant, R.J. Kirkpatrick, MRS Bull. (November 1998) 63.
[22] B.C. Sales, R.S. Ramsey, J.B. Bates, L.A. Boatner, J. Non-Cryst. Solids 87 (1986) 137.
[23] J. Hudgens, R.K. Brow, D.R. Tallatant, S.W. Martin, J. Non-Cryst. Solids 223 (1998) 21.
[24] X. Fang, C.S. Ray, A. Mogus-Milankovic, D.E. Day, J. Non-Cryst. Solids 200 (2001) 162.
[25] R.K. Brow, D.R. Tallant, S.T. Myers, C.C. Phifer, J. Non-Cryst. Solids 191 (1995) 45.
[26] Y.M. Moustafa, K. El-Egili, J. Non-Cryst. Solids 240 (1998) 144.
[27] S. Califano, Vibrational States, Wiley, New York, 1976.
[28] J.R. Ferraro, K. Nakamoto, Introductory Raman Spectroscopy, Academic Press, London, 1994.
[29] R. Berger, J.C. Bissey, J. Kliava, B. Soulard, J. Magn. Magn. Mater. 167 (1997) 129.
[30] R. Berger, J.C. Bissey, J. Kliava, H. Daubric, C. Estournès, J. Magn. Magn. Mater. 234 (2001) 535.

In Fig. 4 (curve a) the vibrational spectra of the crystallized sample are depicted. As expected, the bands have smaller widths compared to the ones in the glass samples, but their position does not differ, which we suggest that after re-heating the sample retained its local structure, i.e., with contribution from both Q^2 and Q^1 species. The complex structure is confirmed by the number of peaks observed below 900 cm^{-1} in the crystallized sample.

The only crystalline phase detected by XRD (Fig. 1) is $Fe_2Pb(P_2O_7)_2$, indicating that the iron valence is +3. No crystalline phases containing ferrous ions have been detected by XRD. Therefore, either part of the Fe^{2+} shown to be present in the as made glass by the Mössbauer spectroscopy oxidized to Fe^{3+} during the crystallization heat treatment, or Fe^{2+} is present in residual amorphous phase. In fact, the Mössbauer spectroscopy for crystalline samples showed that the initial amount of Fe^{2+} in the glass (~19%) is decreased to approximately 8% after crystallization. It is interesting to notice that the Raman bands for the crystalline samples do not change the position compared to the glass samples, but just become sharper.

The IR band at ~500 cm^{-1} is described as a fundamental frequency of Q^0 species or as harmonics of P–O bending vibration [23]. The IR band at 748 cm^{-1} may be attributed to the symmetric vibration of O–P–O rings [26]. The absorption band at ~910 cm^{-1} is attributed to asymmetric stretching vibration of P–O–P groups linked with linear metaphosphate chain [26]. The band at 1118 cm^{-1} may be attributed to a shift in the position of a band at 1130 cm^{-1} assigned to asymmetric stretching between phosphorus and nonbridging oxygen, and an indication for the formation of the terminal phosphate groups PO_3^{2-}. The absorption band at 1228 cm^{-1} may be assigned to asymmetric vibration of Q^2 groups.

The IR spectra for glass and crystalline samples in Figs. 3 and 4, respectively, show bands at the same position. However, the absorption bands of the crystalline sample have smaller widths because of the higher local symmetry.

By comparing the Raman scattering spectrum with the IR absorbance spectrum for glass samples (Fig. 3), bands located in similar positions can be observed, which is a characteristic of low symmetry materials [27]. For the crystalline sample (Fig. 4), the position of most Raman and IR bands do not coincide indicating a higher symmetry (the selection rules for IR and Raman spectroscopy are not the same) [28].

The presence of Q^1 species detected by the Raman spectroscopy is confirmed in the IR spectrum, where the IR bands around 917 and 748 cm^{-1} correspond to asymmetrical and symmetrical P–O–P stretching modes, respectively [24].

A possible explanation is that the addition of Pb^{2+} depolymerizes a number of phosphorous–oxygen chains formed by Q^2 and terminated by Q^1 species [25].

The structure of the LIP glass can be visualized as consisting of PO_4 tetrahedral joined together by oxygen polyhedral which contain Fe(II), Fe(III) and lead ions. The O/P ratio of the $43.3PbO \cdot 13.7Fe_2O_3 \cdot 43P_2O_5$ glass is 3.5, which is the same as that in the lead-free $40Fe_2O_3 \cdot 60P_2O_5$ glass.

The lead free iron phosphate glass previously studied [8,24] has been found to contain PO_4 tetrahedrons joined by one P–O–P bond to form a Q^1 group. The presence of Q^1 groups indicates that the majority of the BO's are due to these groups, in this type of glass.

The X-ray results of crystallized samples indicated that the P_2O_7 groups are bonded to the oxygen polyhedrons that contain the iron and lead ions considered above.

Although the EPR single component of $g = 1.954 \pm 0.002$ (Figs. 5 and 6) is somewhat unusual for Fe^{3+} clusters, that component was attributed to Fe^{3+} ions located outside of the well known sites of single diluted Fe^{3+} ions related to $g = 4.3$, and pairs of $g \sim 2.0$, which were not observed in the present spectrum.

All the Fe^{3+} ions are not constrained to central positions of tetrahedral and octahedral sites of the glass formers; they appear outside at 'interstitial' positions of the structural network and are free to be gathered at distances sufficiently small to be coupled by exchange interactions and their energy levels are split by non-crystal (random) electric field. Analogous changes in magnetic resonance, known as superparamagnetic resonance, were recently reported [29,30].

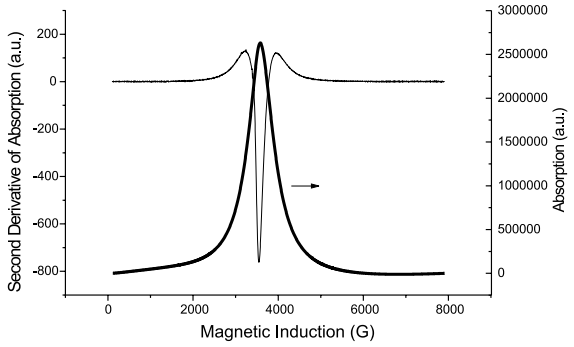

Fig. 6. EPR spectrum of the powdered LIP: absorption and second derivative curves.

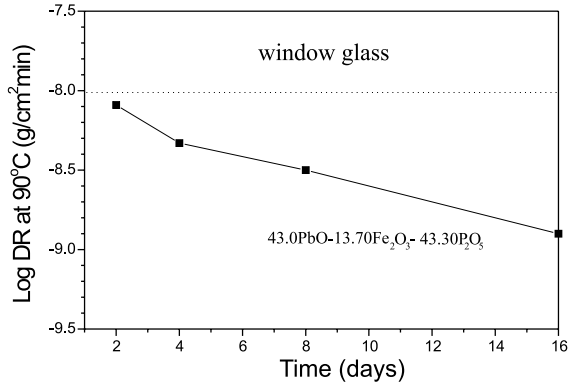

Fig. 7. Dissolution rate for LIP glass as a function of immersion time in aqueous solution at 90 °C. (Lines were drawn as guide for the eye.)

4. Discussion

Models of phosphate glass dissolution in aqueous solutions were studied by Bunker et al. [18]. Experimental dissolution rates for iron phosphate glasses were reported by Day et al. [14]. In the present work, the dissolution rate for the $43.3PbO \cdot 13.7Fe_2O_3 \cdot 43P_2O_5$ glass decreases as the time of immersion in water increases. This decrease is observed in this type of glass because in the early stages the solution is still dilute and the increase of glass leaching products has a relatively minor effect upon the rate of reaction. As the reaction proceeds, the build-up of corrosion products in solution begins to affect the rate of glass reaction. Secondary phases precipitated on the glass surface can decrease the corrosion rate and inhibit mass transfer from the glass to solution [1]. We assumed for this glass the same mechanism of corrosion inhibition. The rate of release of glass components also varies over time and depends on the glass composition, solution, temperature, and presence or absence of crystalline phases [14]. The pH is reduced as a function of time as reported elsewhere for phosphate glasses containing iron [19], leading to lower dissolution rates. The dissolution rate of this LIP glass is less than that usually found for window glasses.

It is well known [20] that the Raman scattering bands in the 1000–1400 cm^{-1} range are ascribed to terminal P–O stretching vibrations and those found in the 600–850 cm^{-1} corresponds to bridging stretching modes [21]. No band is observed at $\approx$1350 cm^{-1} indicating the absence of P=O stretching vibration thus the structure of this glass cannot be described as a P_2O_5 based glass. When the Q^1 tetrahedrons are the majority species in iron phosphate glasses, a strong and broad band appears at 1080 cm^{-1} in the Raman spectrum [22]. On the other hand, the dominance of Q^2 species causes a band at 1200 cm^{-1} [7]. In the region of BO vibrations, the peak at 705 cm^{-1} is asymmetric indicating the overlap of two or more bands. This overlay is expected to occur if Q^2 and Q^1 species are present [22]. Accordingly, the observed IR and Raman scattering spectra are representative of a mixture of chain-terminating Q^1 species and chain-forming Q^2 species.

The addition of iron to lead metaphosphate glasses causes an asymmetric broadening of the Raman scattering band at 1150 cm^{-1}, assigned to symmetric vibration of phosphorus and nonbridging oxygen too [22]. The band at 1130 cm^{-1} in Fig. 3 (curve A) is assigned to this vibration mode if the influence of iron is considered. The 705 cm^{-1} band can be assigned to the symmetrical P–O–P stretching vibrations involving BOs [22]. The band at 500 cm^{-1} has been assigned to the overlapping vibrations involving iron oxygen polyhedral and P_2O_7, which is a characteristic of a structure dominated by Q^1 tetrahedrons [22]. Low frequency bands (340 cm^{-1}) are due to bending modes of the branched and chain network [7]. No Raman bands that could be assigned to Q^0 species were observed [24,25].

Table 1
Room temperature Mössbauer hyperfine parameters, isomer shift (δ) and quadrupole splitting (ΔE_Q), and fraction of ions estimated from the resonance absorption area

	$\langle\delta\rangle$ (mm/s)	$\langle\Delta E_Q\rangle$ (mm/s)	Fraction (%)
Fe^{2+}	1.18 ± 0.03	2.40 ± 0.03	19.15
Fe^{3+}	0.40 ± 0.03	0.88 ± 0.03	80.85

the Mössbauer spectroscopy measurements for a crystallized sample, the fractions of Fe^{2+} and Fe^{3+} were determined to be 8.31% and 91.69%, respectively.

3.3. Vibrational spectroscopies

Fig. 3 shows the Raman scattering spectrum (curve a) and the IR absorbance spectrum (curve b) for the LIP glass. The Raman spectrum for the LIP glass shown contains a feature centered at 1130 cm^{-1}, with shoulders at 1080 and 1230 cm^{-1}. Other bands are found at 340, 500, 705 and 923 cm^{-1}. In the IR spectrum for the LIP glass, bands are observed at 507, 748, 910, 1118 and 1228 cm^{-1}.

Fig. 4 shows the Raman scattering spectrum (curve a) and the IR absorbance spectrum (curve b) for the crystallized sample, for comparison.

3.4. EPR

The EPR spectrum, Fig. 5, was obtained from powder samples of LIP glasses and consists of a single symmetric component centered at $g = 1.954 \pm 0.002$, of derivative p–p width $\Delta B = (36.5 \pm 0.1)$ mT. A small asymmetric feature on the smaller magnetic field side could be detected from the integrated EPR spectrum, confirmed by the small difference between the two maxima of the second derivative of the absorption (Fig. 6). The ratio of the EPR line slopes is equal to six, higher than the slope four of the Lorentzian curve [17].

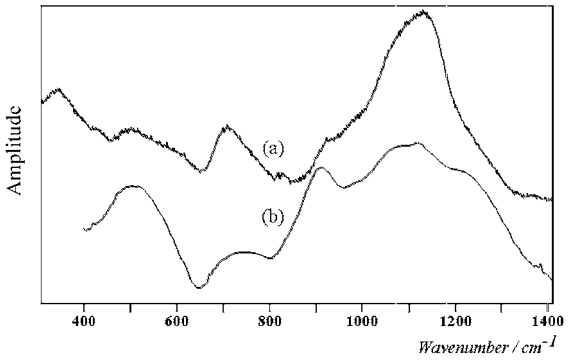

Fig. 3. Raman (curve a) and IR spectra in absorbance (curve b) of a LIP glass $43.3PbO \cdot 13.7Fe_2O_3 \cdot 43P_2O_5$.

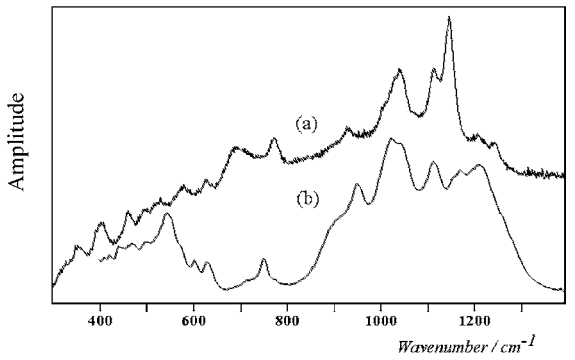

Fig. 4. Raman (curve a) and IR spectra in absorbance (curve b) of a crystallized sample.

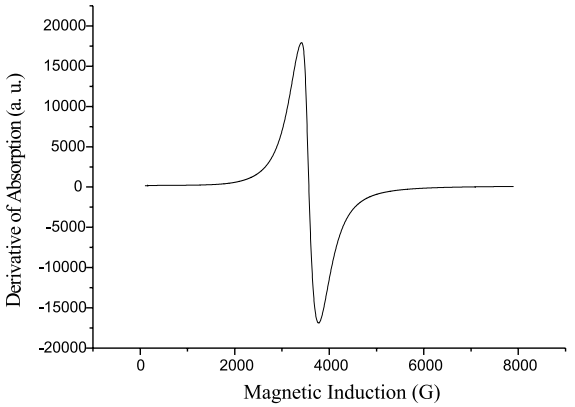

Fig. 5. EPR spectrum of the powdered LIP glass: first derivative curve.

3.5. Dissolution rate

Fig. 7 shows the dissolution rate for LIP glasses as a function of time. The dotted line denotes the dissolution rate for window glass which is included for comparison.

sample between two lucite plates. The amount of iron in the sample was 4 mg/cm^2. The velocity of the source was calibrated using a pure iron foil that was also used as a reference for the isomer shift.

The infrared (IR) spectra of the samples were measured in the range of 450–1500 cm^{-1} by the standard KBr pellet method [16] and as a dispersion in mineral oil, using a Fourier transform infrared (FTIR) spectrometer with an 'Arid Zone', where the sample holder and the peripheral compartments are continuously purged with nitrogen. The pellets were prepared by mixing about 4 mg of glass powder with 150 mg of anhydrous KBr. The KBr was previously dried at 350 °C in an oven and kept in a humidity free environment. During the sample preparation, an IR source was used to keep the sample dry after mixing with KBr.

The Raman spectra of the glass were taken at room temperature coupled to a metallurgical microscope. The spectra were obtained by exciting at 632.8 nm with a He–Ne laser and recorded in the 200–1800 cm^{-1} range. EPR spectra of powdered samples were taken with a homodyne, X-band spectrometer.

The chemical durability of glass samples was measured by the weight loss of samples of $1 \times 1 \times 1$ cm^3 immersed in deionized water at 90 °C for 2–16 days. The samples were polished to 600 grit finish with SiC paper, cleaned with acetone and suspended in glass flasks containing 100 ml of deionized water at 90 °C. Duplicate measurements were made for each glass and the average dissolution rate (D_R), normalized to the glass surface area and the corrosion time, was calculated from the weight loss measured at various times.

3. Results

3.1. X-ray diffraction

Fig. 1 shows the X-ray diffraction pattern of a crystallized sample with composition $43.3PbO \cdot 13.7Fe_2O_3 \cdot 43P_2O_5$. This diffraction pattern indicates that the crystalline phase $Fe_2Pb\ (P_2O_7)_2$ is present [16]. This phase was also identified by using the JCPDS files. The density of the LIP glass is 5.20 ± 0.01 g/cm^3.

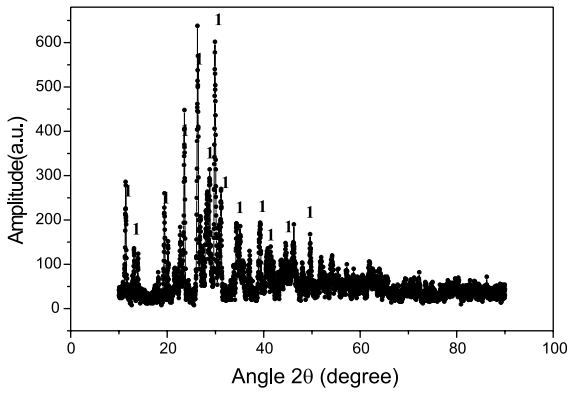

Fig. 1. X-ray diffraction pattern for LIP crystalline sample: 1-peaks due to crystalline $Fe_2Pb(P_2O_7)_2$.

3.2. Mössbauer

The Mössbauer spectrum for the LIP glass measured at room temperature, is shown in Fig. 2. It consists of four partially overlapping lines, related to two doublets, which were computer fitted with Lorentzian lines. The hyperfine parameters, isomer shift (δ) and quadrupole splitting (ΔE_Q), and the fraction of ions estimated from the resonance absorption area are given in Table 1. The isomer shift for Fe^{2+} and Fe^{3+} ions are 1.18 and 0.40 mm/s, respectively, while the quadrupole splitting are 2.40 and 0.88 mm/s, respectively. It is found that some of the Fe^{3+} ions in the starting batch are reduced to Fe^{2+} ions after melting as determined from the Mössbauer spectrum. From

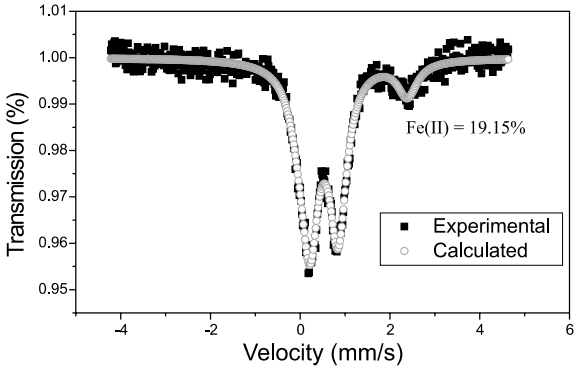

Fig. 2. Mössbauer spectrum obtained at room temperature for the $43.3PbO \cdot 13.7Fe_2O_3 \cdot 43P_2O_5$ glass.

iron to lead phosphate glass was found to increase the chemical durability of the glass and to suppress the tendency for crystallization on cooling or reheating [3]. For sintered lead iron phosphate (LIP) glasses the corrosion rates are $\sim 10^{-2}$ g m^{-2} d^{-1} in distilled water after 28 days corrosion test at 90 °C [4].

The physical and chemical properties of LIP glasses can be modified by varying the melting conditions and composition. In addition to the glass former, P_2O_5, and glass modifier, PbO, Fe_2O_3 is added to increase the chemical durability and the crystallization resistance [5,6]. The structure of an ultraphosphate glass is based on cross-linked chains of tetrahedral PO_4 sharing their corners, each tetrahedron having three bridging oxygen (BO) and one non-bridging oxygen (NBO), thereby satisfying the +5 valence of phosphorus [7]. The addition of PbO results in the creation of NBOs at the expense of BOs [5]. The change from BOs to NBOs with increasing Fe_2O_3 content [6] affects various glass properties. Decrease of the thermal expansion coefficient and the chemical dissolution rate, and increase of the softening temperature have been observed when the Fe_2O_3 content is increased [5–8]. However, based on Mössbauer measurements, it is assumed [5] that Fe^{2+} and Fe^{3+} ions occupy the interstitial glass network sites with octahedral coordination and are not glass formers, which may explain why the absorption bands of Fe–O vibrations are absent in the IR spectra of $40Fe_2O_3 \cdot 60P_2O_5$ glasses [8]. On the other hand, the iron could be detected by electron paramagnetic resonance (EPR) in the glass matrix as Fe^{3+} ions occupying substitutional and interstitial sites in the glass network [9–11], and Fe^{2+} ions, dimers and clusters containing more than two Fe ions are found in the interstitial positions. Even though the reasons for increased chemical durability of iron phosphate glasses are not known, the expected increased hydration resistance of the P–O–Fe links has been cited as a possible reason [12].

Lead free iron–phosphate glasses were also investigated elsewhere with chemical durability improvements [13,14]. Therefore, it seems that there is a controversy if lead should or should not be used in iron phosphate glasses for wasteform application, and on the role of iron in the inhibition of corrosion.

The effects of iron on the structure and chemical stability of several LIP glasses were previously investigated using Mössbauer, EPR, Raman scattering and infrared spectroscopy [15]. Although Raman bands have been attributed to the vibration of PO_2 groups and P–O–P vibration between adjacent PO_4 tetrahedrons, a complete understanding of the origin of many features in the Raman spectra is still lacking to our knowledge. Knowledge of the structure of these glasses may indicate modification of compositions, and processing conditions, which could expand applications.

The aim of the present work was to investigate the structure of the $43.3PbO \cdot 13.7Fe_2O_3 \cdot 43P_2O_5$ (mol%) LIP glass which has a dissolution rate in water of 1.26×10^{-9} g/cm^{-2} min^{-1}, is a potential candidate for use in wasteforms and has the same O/P ratio, 3.5, as the lead-free $40Fe_2O_3 \cdot 60P_2O_5$ glass. X-ray diffraction, Mössbauer, EPR, infrared and Raman scattering spectroscopy were performed and compared to spectra obtained after crystallization.

2. Experimental procedure

The LIP glass with composition $43.3PbO \cdot 13.7Fe_2O_3 \cdot 43P_2O_5$ (mol%) was produced by melting batches of 12.18 wt% Fe_2O_3 (99.97% pure), 53.82 wt% PbO (99.98% pure), and 55.09 wt% $NH_4H_2PO_4$ (Fisher—99.98% pure) in dense alumina crucibles in air at 1100 °C for 1 h. The liquid was quenched in air by pouring it into $1 \times 1 \times 5$ cm^3 steel mold. The samples were transferred to a furnace and annealed at 450 °C for 3 h. The density of the glass was measured by the Archimedes method using distilled water as the immersion liquid. Some samples were crystallized by heating at 700 °C for 24 h. Room temperature X-ray powder diffraction (XRD) data for both glassy and crystalline samples were collected with an X-ray diffractometer.

The Mössbauer spectrum was obtained at room temperature, with a conventional constant-acceleration spectrometer in a 10 mC Rh (^{57}Co) source. The absorber unit was prepared by pressing the powder

ELSEVIER

Journal of Non-Crystalline Solids 304 (2002) 188–194

JOURNAL OF NON-CRYSTALLINE SOLIDS

www.elsevier.com/locate/jnoncrysol

Structural features of lead iron phosphate glasses

S.T. Reis [a], D.L.A. Faria [b], J.R. Martinelli [c,*], W.M. Pontuschka [d], D.E. Day [a], C.S.M. Partiti [d]

[a] *Graduate Center for Materials Research, University of Missouri-Rolla, MO 65409, USA*
[b] *Institute of Chemistry, University of Sao Paulo, C.P. 26077, 05513-970 São Paolo, SP, Brazil*
[c] *Energy and Nuclear Research Institute, Brazilian Nuclear Energy Commission, C.P. 11049 Pinheiros, 05422-970 Sao Paulo, SP, Brazil*
[d] *Institute of Physics, University of São Paulo, C.P. 66318, 05315-970, São Paolo, SP, Brazil*

Abstract

Lead iron–phosphate glasses were investigated for use as wasteform because of their improved chemical durability. There is a controversy if lead should or should not be used in iron phosphate glasses, and on the role of Fe in the inhibition of corrosion. The structure of the $43.3PbO \cdot 13.7Fe_2O_3 \cdot 43P_2O_5$ (mol%) glass, which has a dissolution rate in aqueous solution at 90 °C of 1.26×10^{-9} g/cm^{-2} min^{-1}, and the same O/P ratio, 3.5, as the lead-free $40Fe_2O_3 \cdot 60P_2O_5$ glass, was investigated. Glass samples were produced by melting batches of Fe_2O_3, PbO, and $NH_4H_2PO_4$ at 1100 °C for 1 h, and pouring the liquid into steel mold. Samples were annealed at 450 °C for 3 h. Some samples were crystallized by heating at 700 °C for 24 h. X-ray diffraction, Mössbauer, EPR, infrared, and Raman scattering spectroscopy were performed and compared to spectra obtained after crystallization. The crystalline phase $Fe_2Pb(P_2O_7)_2$ was identified after crystallization. The hyperfine parameters from the Mössbauer spectrum indicates that Fe^{2+} and Fe^{3+} ions are in octahedral coordination, and some of the Fe^{3+} ions in the starting batch are reduced to Fe^{2+} ions after melting. The infrared and Raman scattering spectra are representative of a mixture of chain-terminating Q^1 species and chain-forming Q^2 species. No Raman bands related to P=O vibrations and Q^0 species were observed. From the EPR measurements it is concluded that all Fe^{3+} ions are not constrained to central positions of tetrahedral and octahedral sites of the glass formers.

1. Introduction

Lead phosphate glasses for the immobilization and disposal of nuclear waste were reported in 1984 [1]. The combination of lead phosphate glasses with various types of simulated nuclear waste showed that it is possible to have a waste-form with a corrosion rate one thousand times less than that one of a comparable borosilicate glass. This effect was only observed when the lead phosphate glass was combined with appropriate simulated wastes [2]. The 30-day corrosion rate of lead phosphate glasses in aqueous solution at 90 °C decreased as the solution pH increases [3]. Corrosion rates of 10^{-3} g m^{-2} d^{-1} can be reached for pH > 4. The presence of iron (a component of the simulated nuclear waste) was primarily responsible for the corrosion resistance of the lead phosphate nuclear waste glass [3]. The addition of

* Corresponding author. Tel.: +55-11 816 9367; fax: +55-11 816 9370.
E-mail address: jroberto@net.ipen.br (J.R. Martinelli).

0022-3093/02/$ - see front matter
PII: S0022-3093(02)01021-9